THE JOURNAL OF PHYSICAL CHEMISTRY Letters

Letter

pubs.acs.org/JPCL

Stability of NNO and NPO Nanotube Crystals

Qi An, Hai Xiao, William A. Goddard, III,* and Xiangying Meng

Materials and Process Simulation Center, California Institute of Technology, Pasadena, California 91125, United States

Supporting Information

ABSTRACT: We combine the USPEX evolution searching method with density functional theory using dispersion corrections (DFT-ulg) to predict the crystal structure of the NNO extended solid at high pressures (from 100 to 500 GPa). We find that the NNO nanotube (with diameter ≈ 2.5 Å) is the most stable form above 180 GPa. We report here the stability, electronic properties, and mechanical properties of this novel nanotube and show that it is stable above 20 GPa. To find a similar structure that might be stable at ambient conditions, we considered the NPO tube and show that it is stable at zero pressure. The NPO phase leads to an insulator to metal transition at 25 GPa, where the PP van der Waals distance approaches the covalent bond distance. The energy content of this NPO nanotube crystal is 10.6 kJ/g, which is 152% higher than that of TNT and 86% higher than that of the HMX energetic material. This is the first example of a structural energetic material, which could have important applications in igniters, incendiaries, screening smoke ammunition, and similar devices. This process illustrates how materials discovery in extreme conditions can be used to discover and stabilize novel structures.

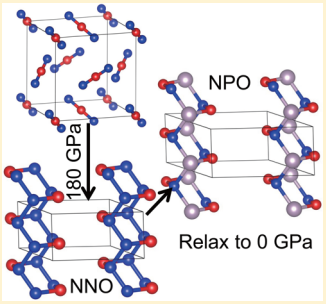

SECTION: Physical Processes in Nanomaterials and Nanostructures

Recently, several examples have been reported of novel three-dimensional materials synthesized by applying high pressure and high temperature to stable gases (e.g., CO, CO_2, N_2, CH_4, NO_2) from the first row of the periodic table. These extended covalent polymeric solids constitute new types of materials that may exhibit such novel properties as high hardness, optical nonlinearity, superconductivity, and high energy density.[1−12] However, there remain major challenges for engineering applications, which requires stabilizing of these novel structures at ambient conditions. For example, at 40 GPa and 1800 K, the CO_2 molecular crystal can be converted to a 3D covalent network that is isomorphic to the β-crystalbalite phase.[3] However, it reverts back to the molecular phase at pressures lower than 1 GPa, despite significant efforts to prevent it.

We showed recently that N_2O (isoelectronic structure to CO_2) forms an extended polymeric solid at high pressures.[13] Previous diamond anvil experiments[14] had found that applying a pressure above 20 GPa and a temperature above 1000 K to N_2O forms a mixture of $(NO^+)(NO_3^-)$ ionic crystal and N_2 molecular crystal. However, we demonstrated[13] using dispersion-corrected density function theory that above 60 GPa, the most stable form of N_2O is a one-dimensional polymer with an all-nitrogen backbone analogous to *cis*-polyacetylene in which alternate nitrogens are covalently bonded to oxygen (a N^+-O^- linkage). More interesting is that below 14 GPa, this high-pressure NNO polymer relaxes to a nonplanar trans polymer that is stable under ambient conditions.[13]

In this Letter, we extended our search for novel materials by examining NNO structures at pressures up to 500 GPa using USPEX evolutionary crystal structure searching combined with density functional theory with dispersion correction (DFT-ulg).[15] Indeed, we predict that above 180 GPa, a novel NNO crystal structure ($P21/m$ space group) consisting of ∼2.5 Å diameter NNO nanotubes is favored. In this structure, each N has single bonds to two N's and one O, while each O is bonded to two N's. Then, we used DFT to predict the phonon spectrum from 0 to 200 GPa, where we found that this new phase is stable above 20 GPa. We examined the electronic properties of the NNO nanotube using DFT, where we found that the band gap increases as the pressure increases to 200 GPa.

Next, we examined how to stabilize the nanotube structure and found that replacing alternate nitrogen atoms by phosphorus atoms leads to a NPO nanotube that is stable at ambient conditions. We then used DFT to predict the stability, electronic properties, and mechanical properties of the NPO nanotube. We found that the NPO nanotube is more stable than the NNO tube and that the NPO nanotube transforms to a metallic phase at 25 GPa.

The evolutionary structure searching was performed using the USPEX[16−18] evolutionary algorithm developed by Oganov, Glass, and Lyakhov, which features local optimization, real space representation, and flexible physically motivated variation operators. Here, we applied the Perdew−Burke−Ernzerhof (PBE) exchange−correlation functional including the low gradient London dispersion correction (PBE-ulg) implemented in the VASP package,[19−21] modified to describe PBE-ulg and using the projector-augmented wave method[22] to account for the core−valence interactions. We found that a kinetic energy cutoff of 1000 eV for the plane wave expansions gives excellent convergence of the total energies, energy differences, and

Received: December 11, 2013
Accepted: January 5, 2014
Published: January 6, 2014

structural parameters at high pressures. Reciprocal space was sampled using the Γ-centered Monkhorst−Pack scheme with a fine resolution of $2\pi \times 1/60$ Å^{-1}. The convergence criteria were set to a 1×10^{-6} eV energy difference for solving the electronic wave function and a 1×10^{-3} eV/Å force for geometry optimization. For faster structure searches using USPEX, the reciprocal grid resolution was lowered to $2\pi \times 0.06$ Å^{-1}.

Figure 1 shows the enthalpy−pressure relations for the lowest-energy structures from the crystal structure search. We

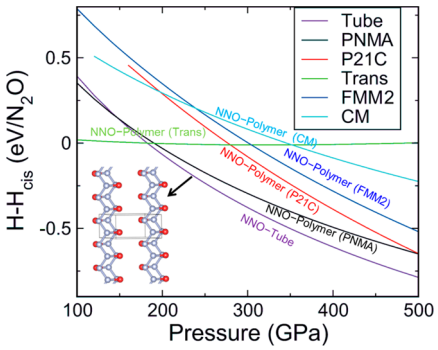

Figure 1. Ground-state enthalpy difference (relative to the one-dimensional cis polymer structure[14]) as a function of pressure for various predicted extended forms of NNO. The NNO nanotube crystal structure (inset) is the most favored above 180 GPa. It can be considered as formed from two parallel NNO trans polymers, −N═(NO)−N═(NO)−N−, that are linked together by reacting across the N═N double bonds. Thus, in the final structure, all N atoms have a lone pair with two single NN bonds and one single NO bond. The *Pnma* structure has the same two parallel NNO trans polymers, −N═(NO)−N═(NO)−N−, aligned appropriate for forming the nanotube but no cross-linking. The *P*21/*c* structure also has two parallel NNO polymers, but the polymer structure is a mixture of cis and trans. The *Fmm*2 structure combines two NNO trans polymers, but one polymer is shifted *b*/2 along the chain direction and linked parallel to the other trans polymer. The *Cm* structure is also formed by linking the NNO trans polymer but with additional N and O atoms.

predict that for pressures above 180 GPa, the one-dimensional NNO cis polymer transforms into the *P*21/*m* space group consisting of 2.5 Å diameter NNO nanotubes. This nanotube can be considered as formed from two parallel NNO trans polymers, −N═(NO)−N═(NO)−N−, which we link together by reacting across the N═N double bonds. Thus, in the final structure, every N atom has a lone pair with two single NN bonds and one single NO bond, as shown in the inset of Figure 1. The two NN bonds have the same bond length of 1.458 Å, which is a normal N−N single bond distance. The unit cell of this novel structure contains six atoms with cell parameters a = 4.43 Å, b = 2.28 Å, c = 4.48 Å, α = 90°, β = 68.4°, and γ = 90°. This leads to a density of 2.44 g/cm^3 compared to 1.52 g/cm^3 for the NNO molecular crystal and 1.72 g/cm^3 for the $(NO^+)(NO_3^-)$ ionic crystal. This nanotube structure is the most stable structure over the pressure range from 180 to 500 GPa.

Between 60 and 180 GPa, the most stable phase is the one-dimensional *cis*-NNO polymer described previously.[13] Above 200 GPa, we found that the two-dimensional NNO polymer structure with *Pnma* space group is favored over the one-dimensional polymers, but it is less stable than the nanotube structure. Beyond 500 GPa, a second two-dimensional polymer with *P*21/*c* space group is more stable than the *Pnma* structure. Structure files for all of these phases are included in the Supporting Information (SI).

To establish crystal stability with respect to soft phonon modes, it is essential to evaluate the phonon spectra. To do this for the predicted nanotube structure, we used very tight convergence criteria, with 1×10^{-10} eV energy difference and 1×10^{-6} eV/Å force thresholds. Here, we calculated the force constants using the supercell approach with finite displacements, as implemented in the PHONOPY code.[23] We found that the phonon dispersion bands have no imaginary modes for pressures between 20 and 200 GPa, as shown in Figure 2a and

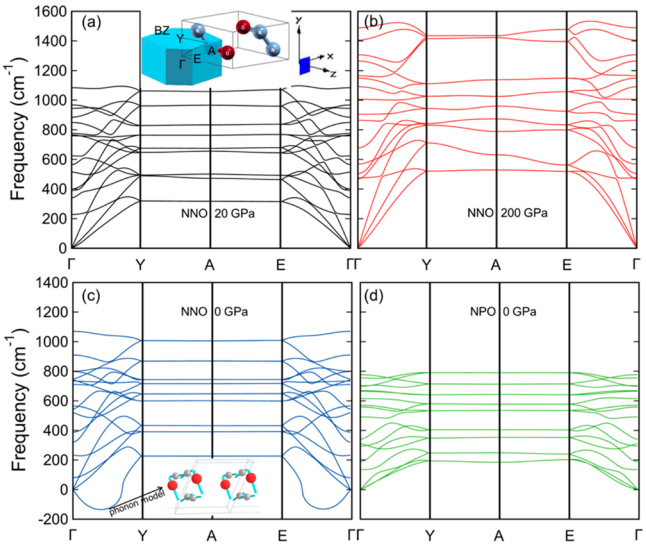

Figure 2. Phonon dispersion curves for the NNO and NPO nanotube structures. (a) NNO at 20 GPa (black line, with the N−O bond vibration at 515−849 cm^{-1}; the inset shows the Brillouin zone). (b) NNO at 200 GPa (red line, with the N−O bond vibration at 678−1149 cm^{-1}). (c) NNO tube at zero pressure (blue line, with the negative eigenmode located at $(0, 0.25, 0) \times 2\pi/b$, corresponding to the dissociation of the nanotube to O═N−N═O and N_2, displayed by the inset). (d) NPO tube at zero pressure (green line with the P−O bond vibration at 577−669 cm^{-1}).

b. This indicates that the NNO nanotube crystal is stable for pressures above 20 GPa. However, below 20 GPa, we find that an imaginary phonon mode appears located at $(0, 0.25, 0) \times 2\pi/b$ in the Brillouin zone. This mode corresponds to dissociating the nanotube into O═N−N═O and N_2, as shown in the inset of Figure 2c, indicating the instability of this structure at zero pressure.

To stabilize the novel nanotube formed by NNO, we considered various changes. In particular, we expected that replacing alternate N in the N−N chain with P to form the −N−(P−O−N)−N−(P−O−N)− backbone would stabilize the N lone pair compared to having N−N bonds in the chain. Indeed, we find that the NPO nanotube crystal structure retains the *P*21/*m* space group, while Figure 2d shows that there are no imaginary phonon modes, indicating that the structure is stable (local minima). The nanotube diameter increases from 2.5 to 2.7 Å, while the cell parameters change to a = 5.69 Å, b = 2.76 Å, c = 5.56 Å, α = 90°, β = 60.9°, and γ = 90°. The two P−N bonds have the same bond length of 1.75 Å, compared to equal N−N bonds of 1.46 Å in the NNO tube. The P−O bond and N−O bond are 1.67 and 1.49 Å, respectively. The PON

dx.doi.org/10.1021/jz402682y | *J. Phys. Chem. Lett.* 2014, 5, 485−489

angle is 115.9°. The inversion angles for the P and N atoms are 49.3 and 69.6°, respectively.

High pressures often transform an insulator to a metallic phase. To examine the electronic properties of the NNO and NPO extended systems, we used the B3PW91 flavor of DFT, which has been established to give accurate band gaps.[24] The B3PW91 calculations were conducted using the CRYSTAL09 package[25] using the 6-311G* triple-ζ quality basis sets. We also include band calculations using the PBE flavor of DFT for comparison. The results are shown in Figure 3, where we see

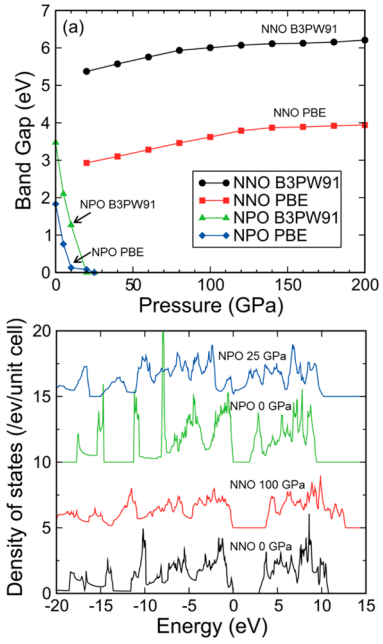

Figure 3. Electronic band gap and density of states (DOS) for NNO and NPO nanotubes under high pressures. (a) Band gap as a function of pressure; (b) electronic DOS at various pressures. The DOS are shifted along the *y* axis to avoid overlaps. Note for NPO the very sharp DOS at −8 eV for 0 pressure, which corresponds to the localized P−O bonds that disappear at 25 GPa because of overlap of these nonbonding electrons.

that the NNO nanotube band gap exhibits an abnormal linear increase from 5.4 to 6.2 eV for B3PW91 (from 2.8 to 4.0 eV for PBE) as the pressure increases to 200 GPa, while for the NPO nanotube, the band gap decreases to 0, leading to metallization at 25 GPa. Figure 3b shows that the electronic density of states (DOS) becomes more extended and flattened for the NNO tube as the pressure increases, leading to the increase in the band gap. However, for the NPO tube, the band gap disappears at 25 GPa. We also included the band structures of the NPO nanotube structure as the function of pressure in Figure S1 of the SI. To explore the origin of this opposite behavior for these similar nanotube structures, we plot the charge density distribution as a function of pressure in Figure 4. For the NNO nanotube, the charge density is confined to the nanotube. It becomes increasingly localized as the pressure increases from 0 to 200 GPa, leading to the increase in band gap.

As the NPO crystal is compressed to 25 GPa, the nonbond distances decrease dramatically, P···P from 3.36 to 2.39 Å, N···P from 3.24 to 2.51 Å, and N···N from 3.36 to 2.73 Å. Thus, at 25 GPa, the P···P nonbond distance is only 8% longer than the P−P single-bond distance of 2.21 Å, which seems to be the origin of the metallic character. The variations of nonbond distances

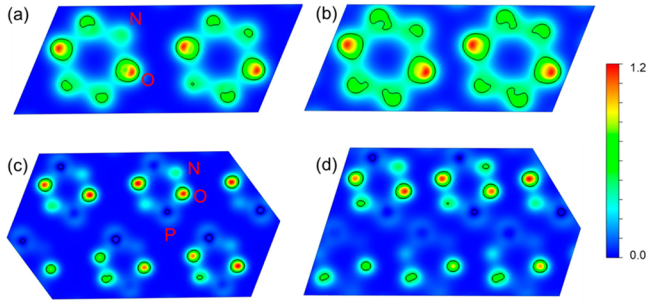

Figure 4. Two-dimensional charge density (e/a_0**3) distribution in NNO and NPO at various pressures. (a) NNO at 20 GPa. (b) NNO at 200 GPa. (c) NPO at 0 GPa. (d) NPO at 25 GPa. The solid black line is the contour at 0.58, the middle value of the charge density.

P···P, P···N, and N···N as the pressure increases are shown in Figure S2 of the SI. For a pressure of 25 GPa, the compression of the nanotube leads to P−O = 1.64 Å, N−O = 1.47 Å, ∠PON = 120.7°, ∠P_inv = 49.6°, and ∠N_inv =71.5°. Because all bonds in the nanotube are single bonds, the lone pairs of the N and P atoms point outside of the nanotube.

To predict the mechanical properties of the NPO nanotube structure at zero pressure, we used DFT-PBE-ulg to calculate the elastic moduli, bulk modulus, and shear modulus at zero temperature. Here, we calculate the elastic moduli from the stress−strain relation as a function of various cell distortions δ from the equilibrium lattice configuration.[26] The resulting elastic moduli are shown in Table 1. Analyzing the elastic

Table 1. Predicted Elastic Moduli (GPa) for the NPO Nanotube Crystal Framework[a]

C_{ijkl}	*XX*	*YY*	*ZZ*	*XY*	*YZ*	*ZX*
XX	29.6	4.8	2.5	0	0	−2.9
YY	4.8	307.8	8.0	0	0	−1.6
ZZ	2.5	8.0	33.2	0	0	−2.9
XY	0	0	0	8.1	−3.6	0
YZ	0	0	0	−3.6	24.0	0
ZX	−2.9	−1.65	−2.9	0	0	6.6

[a]The chain axis is *y*. Some of the off-diagonal moduli are negative, as is common for a monoclinic crystal structure.

moduli using the Voigt method[27] leads to a bulk modulus of B = 44.6 GPa and shear modulus of G = 31.4 GPa. The elastic modulus along tube direction is c_{22} = 307.8 GPa, which can be compared to 642 GPa for a carbon single-walled nanotube rope (4.5 nm).[28] Because G/B = 0.7 < 1.0, we expect the NPO nanotube to be a brittle material.[29]

Our unit cell for the NPO polymer has just one single nanotube, which fixes the relative orientation of adjacent nanotubes. To determine whether there might be better packing structures, we considered the 2 × 2 × 2 supercell and calculated the potential energy curve for rotating the adjacent tubes counterclockwise. Figure S3 of the SI shows several local minimum structures in the potential energy curve. The best structure denoted as NPO_R has the conformation formed by rotating the adjacent nanotube 60° clockwise. It has an energy 0.03 eV lower than our original structure. The original orientation tube structure (named NPO) is the second best structure among all of these conformations. We calculated an energy barrier of 0.2 eV for transforming from the NPO structure to the NPO_R structure

dx.doi.org/10.1021/jz402682y | J. Phys. Chem. Lett. 2014, 5, 485−489

We also calculated the equation of states and electronic properties of the new NPO_R structure and compared with the NPO structure in Figure S4 (SI) (enthalpy of NPO and NPO_R structures as a function of pressure) and Figure S5 (SI) (the band gap and electronic DOS of the NPO_R nanotube). These results indicate that the NPO structure is more favorable for pressures above 10 GPa, with the difference increasing with pressure. Figure S5 of SI shows that the NPO_R experiences an insulator to metallic phase transition for pressures above 60 GPa, which is also induced by the overlap of P lone pairs between adjacent nanotubes.

The PNO molecule was first observed experimentally in an argon matrix.[30] Later, it was detected in the gas phase by infrared laser absorption spectroscopy.[31] The stabilities of the isomers PNO, NOP, and NPO and their corresponding anions and cations were investigated using high-level ab initio coupled cluster CCSD methodology.[32] These studies found that NPO is the most stable isomer, but PNO is only 1.7 kcal/mol higher in energy (PON is much higher in energy by 29.9 kcal/mol). Our predicted NPO nanotube could be synthesized from either PNO or NPO species by reacting across the P═N, P═O, and N═O double bonds.

Phosphorus is widely used in military applications as igniters, incendiaries, screening smoke ammunition, flames, and smoke signals because of its high reactivity toward oxygen, its high enthalpy of combustion, and the impressive obscuring power.[33] The energy content of the NPO nanotube crystal is 10.6 kJ/g, considering that it reacts with O_2 to form N_2 and P_2O_5, which is 152% higher than that of TNT (4.2 kJ/g) and 86% higher than that of the HMX (5.7 kJ/g) energetic materials. Thus, the NPO nanotube could have potential important applications as a structural high-energy-content energetic material.

Summarizing, we predict that a novel NNO nanotube (with diameter ≈ 2.5 Å) crystal ($P21/m$ space group) is the most stable form of NNO from 180 to 500 GPa. The predicted phonon spectrum validates the stability of this novel structure for pressures over 20 GPa. The band gap of this nanotube shows an abnormal increase with pressure up to 500 GPa.

To stabilize the nanotube structure at zero pressure, we examined high-pressure forms of the NPO molecule. We find that the NPO nanotube is stable at ambient conditions, leading to an insulator to metal transition at 25 GPa.

■ ASSOCIATED CONTENT

Supporting Information

The nonbond distances P···P, P···N, and N···N of the NPO tube as a function of pressure, the band structure of the NPO tube as a function of pressure, the potential energy curve of nearby nanotube rotation, the equation of states of NPO and NPO_R tube structures, and the electronic properties of the NPO_R structure. It also includes the cif files from the evolution search of the NNO extended solid and for the stable form of NPO and NPO_R at ambient pressure. This material is available free of charge via the Internet at http://pubs.acs.org.

■ AUTHOR INFORMATION

Corresponding Author

*E-mail: wag@wag.caltech.edu.

Notes

The authors declare no competing financial interest.

■ ACKNOWLEDGMENTS

This work was supported by the Defense Advanced Research Projects Agency (W31P4Q-13-1-0010, program manager, Judah Goldwasser).

■ REFERENCES

(1) Mailhiot, C.; Yang, L. H.; McMahan, A. K. Polymeric Nitrogen. *Phys. Rev. B* **1992**, *46*, 14419−14435.
(2) Eremets, M. I.; Gavriliuk, A. G.; Trojan, I. A.; Dzi-venko, D. A.; Boehler, R. Single-Bonded Cubic Form of Nitrogen. *Nat. Mater.* **2004**, *3*, 558−563.
(3) Iota, V.; Yoo, C. S.; Cynn, H. Quartzlike Carbon Dioxide: An Optically Nonlinear Extended Solid at High Pressures and Temperatures. *Science* **1999**, *283*, 1510−1513.
(4) Serra, S.; Cavazzoni, C.; Chiarotti, G. L.; Scandolo, S.; Tosatti, E. Pressure-Induced Solid Carbonates from Molecular CO_2 by Computer Simulation. *Science* **1999**, *284*, 788−790.
(5) Bernard, S.; Chiarotti, G. L.; Scandolo, S.; Tosatti, E. Decomposition and Polymerization of Solid Carbon Monoxide under Pressure. *Phys. Rev. Lett.* **1998**, *81*, 2092−2095.
(6) Lipp, M. J.; Evans, W. J.; Baer, B. J.; Yoo, C. S. High-Energy-Density Extended CO Solid. *Nat. Mater.* **2005**, *4*, 211−215.
(7) Pickard, C. J.; Needs, R. J. Highly Compressed Ammonia Forms an Ionic Crystal. *Nat. Mater.* **2008**, *7*, 775−779.
(8) Ciabini, L.; Santoro, M.; Gorelli, F. A.; Bini, R.; Schettino, V.; Raugei, S. Triggering Dynamics of the High-Pressure Benzene Amorphization. *Nat. Mater.* **2007**, *6*, 39−43.
(9) McMillan, P. F. New Materials from High-Pressure Experiments. *Nat. Mater.* **2002**, *1*, 19−25.
(10) Datchi, F.; Mallick, B.; Salamat, A.; Ninet, S. Structure of Polymeric Carbon Dioxide CO_2-V. *Phys. Rev. Lett.* **2012**, *108*, 125701.
(11) Yoo, C. S.; Cynn, H.; Gygi, F.; Galli, G.; Iota, V.; Nicol, M.; Carlson, S.; Häusermann, D.; Mailhiot, C. Crystal Structure of Carbon Dioxide at High Pressure: "Superhard" Polymeric Carbon Dioxide. *Phys. Rev. Lett.* **1999**, *83*, 5527−5530.
(12) Dong, J. J.; Tomfohr, J. K.; Sankey, O. F.; Leinenweber, K.; Somayazulu, M.; McMillan, P. F. Investigation of Hardness in Tetrahedrally Bonded Nonmolecular CO_2 Solids by Density-Functional Theory. *Phys. Rev. B* **2000**, *62*, 14685−14689.
(13) Xiao, H.; An, Q.; Goddard, W. A., III; Liu, W. G.; Zybin, S. V. Formation of the −N(NO)N(NO)− Polymer at High Pressure and Stabilization at Ambient Conditions. *Proc. Natl. Acad. Sci. U.S.A.* **2013**, *110*, 5321−5325.
(14) Somayazulu, M.; Madduri, A.; Goncharov, A. F.; Tschauner, O.; McMillan, P. F.; Mao, H. K.; Hemley, R. J. Novel Broken Symmetry Phase from N_2O at High Pressures and High Temperatures. *Phys. Rev. Lett.* **2001**, *87*, 135504.
(15) Kim, H.; Choi, J. M.; Goddard, W. A., III. Universal Correction of Density Functional Theory to Include London Dispersion (up to Lr, Element 103). *J. Phys. Chem. Lett.* **2012**, *3*, 360−363.
(16) Oganov, A. R.; Glass, C. W. Crystal Structure Prediction Using *Ab Initio* Evolutionary Techniques: Principles and Applications. *J. Chem. Phys.* **2006**, *124*, 244704.
(17) Glass, C. W.; Oganov, A. R.; Hansen, N. USPEX—Evolutionary Crystal Structure Prediction. *Comput. Phys. Commun.* **2006**, *175*, 713−720.
(18) Lyakhov, A. O.; Oganov, A. R.; Valle, M. How to Predict Very Large and Complex Crystal Structures? *Comput. Phys. Commun.* **2010**, *181*, 1623−1632.
(19) Kresse, G.; Hafner, J. Ab Initio Molecular Dynamics for Liquid Metals. *Phys. Rev. B.* **1993**, *47*, 558−561.
(20) Kresse, G.; Furthmuller, J. Efficiency of Ab-Initio Total Energy Calculations for Metals and Semiconductors Using a Plane-Wave Basis Set. *Comput. Mater. Sci.* **1996**, *6*, 15−50.
(21) Kresse, G.; Furthmüller, J. Efficient Iterative Schemes for *Ab Initio* Total-Energy Calculations Using a Plane-Wave Basis Set. *Phys. Rev. B* **1996**, *16*, 11169−11186.

(22) Kresse, G.; Joubert, D. From Ultrasoft Pseudopotentials to the Projector Augmented-Wave Method. *Phys. Rev. B* **1999**, *59*, 1758−1775.
(23) Togo, A.; Oba, F.; Tanaka, I. First-Principles Calculations of the Ferroelastic Transition between Rutile-Type and $CaCl_2$-Type SiO_2 at High Pressures. *Phys. Rev. B* **2008**, *78*, 134106.
(24) Xiao, H.; Tahir-Kheli, J.; Goddard, W. A., III. Accurate Band Gaps for Semiconductors from Density Functional Theory. *J. Phys. Chem. Lett.* **2011**, *2*, 212−217.
(25) Dovesi, R.; Saunders, V. R.; Roetti, C.; Orlando, R.; Zicovich-Wilson, C. M.; Pascale, F.; Civalleri, B.; Doll, K.; Harrison, N. M.; Bush, I. J.; et al. *CRYSTAL 2009 User's Manual*; University of Torino: Torino, Italy, 2009.
(26) Le Page, Y.; Saxe, P. Symmetry-General Least-Squares Extraction of Elastic Data for Strained Materials from *Ab Initio* Calculations of Stress. *Phys. Rev. B* **2002**, *65*, 104104.
(27) Chung, D. H. Elastic Moduli of Single Crystal and Polycrystalline MgO. *Philos. Mag.* **1963**, *8*, 833−841.
(28) Salvetat, J. P.; Briggs, G. A. D.; Bonard, J. M.; Bacsa, R. R.; Kulik, A. J.; Stöckli, T.; Burnham, N. A.; Forró, L. Elastic and Shear Moduli of Single-Walled Carbon Nanotube Ropes. *Phys. Rev. Lett.* **1999**, *82*, 944−947.
(29) Pugh, S. F. Relations between the Elastic Moduli and the Plastic Properties of Polycrystalline Pure Metals. *Philos. Mag.* **1954**, *45*, 823−843.
(30) Ahlrichs, R.; Schunck, S.; Schnockel, H. Structure of Molecular PNO, Matrix Isolation and Ab Initio Calculation. *Angew. Chem., Int. Ed. Engl.* **1988**, *27*, 421−423.
(31) Bell, I. S.; Hamilton, P. A.; Davies, P. B. Detection of the Transient PNO Molecule by Infrared Laser Absorption Spectroscopy. *Mol. Phys.* **1998**, *94*, 685−691.
(32) Grant, D. J.; Dixon, D. A.; Kemeny, A. E.; Francisco, J. S. Structures and Heats of Formation of the Neutral and Ionic PNO, NOP, and NPO Systems from Electronic Structure Calculations. *J. Chem. Phys.* **2008**, *128*, 164305.
(33) Koch, E. C. Special Materials in Pyrotechnics: V. Military Applications of Phosphorus and its Compounds. *Propellants, Explosives, Pyrotechnics* **2008**, *33*, 165−176.